

Keywords: gastric cancer; FOXO1; HER2; tumour growth; metastasis

Loss of FOXO1 promotes gastric tumour growth and metastasis through upregulation of human epidermal growth factor receptor 2/neu expression

Young San Ko¹, Sung Jin Cho¹, Jinju Park², Younghoon Kim³, Yong Joon Choi⁴, Jung-Soo Pyo⁵, Bo Gun Jang⁶, Jong-Wan Park^{4,7}, Woo Ho Kim³ and Byung Lan Lee^{*,1,2,7}

¹Department of Anatomy, Seoul National University College of Medicine, 103 Daehak-ro, Jongno-gu, Seoul 110-799, South Korea;

²Tumour Biology (Cancer Research Institute), Seoul National University College of Medicine, Seoul 110-799, South Korea;

³Department of Pathology, Seoul National University College of Medicine, Seoul 110-799, South Korea; ⁴Department of

Pharmacology, Seoul National University College of Medicine, Seoul 110-799, South Korea; ⁵Department of Pathology, Kangbuk

Samsung Hospital, Sungkyunkwan University School of Medicine, Seoul 110-746, South Korea; ⁶Department of Pathology, Jeju

National University Hospital, Jeju 690-767, South Korea and ⁷Ischemic/Hypoxic Disease Institute Medical Research Center, Seoul

National University College of Medicine, Seoul 110-799, South Korea

Background: The biological significance of FOXO1, a member of the forkhead box O transcription factor family, in gastric cancer (GC) remains unclear. The present study provides direct evidence of the role of FOXO1 in tumour growth and metastasis of GC in relation to human epidermal growth factor receptor 2 (HER2).

Methods: The expressions of FOXO1 and HER2 were modulated in GC cell lines (SNU-638, MKN45, SNU-216 and NCI-N87) by stable transfections. The effects of transfection on GC phenotypes were evaluated *in vitro* and in animal models. In addition, the relationship between FOXO1 and HER2 was analysed using GC clinical specimens, cell lines and xenografts.

Results: FOXO1 silencing in GC cells increased colony formation and mesenchymal transition *in vitro*, as well as tumour growth and metastasis in nude mice, whereas HER2 silencing induced the opposite results. Furthermore, an inverse relationship between FOXO1 and HER2 was found in clinical specimens of GC, GC cells and GC xenograft tumours. Although a negative crosstalk between these two molecules was shown, double knockdown of both FOXO1 and HER2 in GC cells revealed that HER2 silencing reversed the FOXO1 shRNA-induced migration and invasion even without the FOXO1 restoration.

Conclusions: Our results indicate that loss of FOXO1 promotes GC growth and metastasis by upregulating HER2 expression and that the HER2 expression is more critical to the induction of GC cell metastasis. The present study provides evidence that the FOXO1/HER2 pathway may regulate GC progression in a subgroup of GC patients.

Gastric cancer (GC) is one of the most common malignant cancers showing multiorgan metastasis when diagnosed in an advanced stage. Since advanced metastatic GC remains largely incurable, identifying key regulators of the malignant

phenotype of GC would help in developing a therapeutic strategy for GC.

FOXO1 is one of the mammalian forkhead transcription factors of class O (FOXO), which is involved in a variety of biological

*Correspondence: Professor BL Lee; E-mail: dslanat@snu.ac.kr

Revised 4 May 2015; accepted 1 July 2015; published online 8 October 2015

© 2015 Cancer Research UK. All rights reserved 0007–0920/15

processes (Feng *et al*, 2011; Kim *et al*, 2015). The FOXO1 protein is tightly regulated by multiple posttranslational modifications, including phosphorylation, acetylation, ubiquitination and methylation, and FOXO1 expression is highly variable in different tissues (van der Horst and Burgering, 2007). In human cancers, FOXO1 decreased metastatic potential through the inhibition of matrix metalloproteinase-7 (MMP7) in larynx cancer cells (Ding *et al*, 2014) or MMP9 in lung cancer cells (Pei *et al*, 2014) and glioblastoma cells (Chen *et al*, 2014). In contrast, FOXO1 led to an increase in the expression of MMP1 followed by breast cancer cell metastasis (Feng *et al*, 2011). Thus, the role of FOXO1 in tumour metastasis and the underlying molecular mechanisms could be cancer cell-type specific. However, little is known about the effect of FOXO1 on the GC cell metastasis.

Human epidermal growth factor receptor 2 (HER2/ErbB2/neu) is a member of the epidermal growth factor receptor family, and is expressed in 6–35% of GC cases (Lin *et al*, 2000) and in 15–59% of advanced GC cases (Bang, 2012). Although HER2 downregulation decreased cancer cell motility and the invasion of GC cells *in vitro* (Bao *et al*, 2010), the underlying molecular mechanisms of HER2-induced GC metastasis need to be elucidated. Earlier *in vitro* studies (Wu *et al*, 2010; Lazrek *et al*, 2013) reported that HER2 expression was inversely correlated with FOXO1 activation in breast cancer cells, but there is no information on this relationship in GC.

Previously, we have reported that the expression of FOXO1 phosphorylated at Ser256 (pFOXO1, inactive form) was frequently found in GC specimens with a prognostic significance (Kim *et al*, 2007). However, the direct evidence of the role of FOXO1 in the context of metastatic behaviours of GC has not been published. In the present study, we investigated the role of FOXO1 in the tumour growth and metastasis of GC *in vitro* and *in vivo*. In addition, we determined the association between FOXO1 and HER2 in GC using human tissue specimens, cell lines and xenografts.

MATERIALS AND METHODS

Cell culture. Five well-characterized human GC cell lines (SNU-216, SNU-484, SNU-638, MKN45 and NCI-N87) were purchased from the Korean Cell Line Bank (Seoul, Korea). Cells were maintained in RPMI 1640 medium (Life Technologies, Grand Island, NY, USA) containing 10% foetal bovine serum (FBS), and incubated in 5% CO₂.

Reagents and antibodies. Antibodies against total FOXO1 (rabbit monoclonal), phospho-FOXO1^{Ser256} (pFOXO1, rabbit polyclonal), HER2 (rabbit monoclonal), phospho-AKT^{Ser473} (pAKT, rabbit polyclonal) and phospho-GSK-3^{Ser9} (pGSK-3 β , rabbit polyclonal) were purchased from Cell Signaling Technology (Beverly, MA, USA). Antibody against E-cadherin (mouse monoclonal) was purchased from BD Biosciences (San Jose, CA, USA). Antibodies against Snail (rabbit polyclonal) and β -actin (mouse monoclonal) and horseradish peroxidase-conjugated secondary antibodies were purchased from Santa Cruz Biotechnology (Santa Cruz, CA, USA). Alexa Fluor-555-conjugated anti-rabbit IgG, Alexa Fluor-488-conjugated anti-mouse IgG and DAPI (4',6-diamidino-2-phenylindole) were purchased from Life Technologies. Alexa Fluor 633-conjugated phalloidin was purchased from Invitrogen (Carlsbad, CA, USA). The phosphoinositide 3-kinase (PI3K) inhibitor LY294002 was purchased from Cell Signaling Technology, and AKT inhibitor IV was purchased from Calbiochem (La Jolla, CA, USA).

Immunoblot analysis. Immunoblot analysis was performed as we described previously (Nam *et al*, 2011). Briefly, cell lysates in SDS lysis buffer (125 mM Tris-HCl (pH 6.8), 4% SDS, 0.004% bromophenol blue, and 20% glycerol) were separated on 10% SDS-polyacrylamide gel and electrophoretically transferred to

PVDF membranes (Millipore Corporation, Billerica, MA, USA) blocked with 5% non-fat dry milk in PBS-Tween-20 (0.1%, vol/vol) for 1 h. The membranes were then incubated with a primary antibody against FOXO1 (1:1000), E-cadherin (1:1000), Snail (1:1000), HER2 (1:1000), pAKT (1:1000), pGSK-3 β (1:1000) or β -actin (1:1000). Horseradish peroxidase-conjugated anti-rabbit IgG (1:2000) or anti-mouse IgG (1:2000) was used as a secondary antibody. Enhanced chemiluminescence (Amersham, Arlington Heights, IL, USA) was used to detect the immunoreactive proteins. Equal protein loading was confirmed by β -actin.

Transfection of FHRE-luciferase construct and luciferase reporter assay. To determine FOXO1 nuclear DNA-binding activity in GC cells, luciferase reporter assay was performed as previously described (Park *et al*, 2014). Gastric cancer cells were seeded in 24-well plates at a density of 3×10^4 cells per well and were transiently cotransfected with 0.4 μ g forkhead responsive element (FHRE)-luciferase reporter plasmid (reporter construct in which a small region of the Fas ligand promoter contains the three FHREs, Addgene plasmid 1789, Addgene Incorp, Cambridge, MA, USA) and 0.4 μ g pSV- β -galactosidase vector (Promega, Madison, WI, USA), an internal control, using Lipofectamine Plus (Life Technologies). Twenty-four hours after transfection, assays for luciferase and β -galactosidase were carried out using a Dual-Luciferase Reporter Assay System (Promega). Luciferase activity was measured on an AutoLumat LB 9505c luminometer (Berthold Analytical Instruments, Nashua, Germany) and was normalised by β -galactosidase activity.

Lentivirus-mediated shRNA silencing of FOXO1 and HER2. Lentiviral particles containing non-targeting short hairpin RNA (shRNA), FOXO1 shRNA or HER2 shRNA were purchased (Sigma, St. Louis, MO, USA). The sequence of FOXO1 shRNA was 5'-CCGGGCTGTTATCAATCTGCTAAACTCGAGTTTACAGATTGATAACAGGCTTTTTG-3', and that of HER2 shRNA was 5'-CCGGTGTCTAGTATCCAGGCTTTGTACTCGAGTACAAAG CCTGGATACTGACATTTTTG-3'. The control shRNA particles contain 4 bp mismatches within the short hairpin sequence to any known human or mouse gene. Viral infection was performed by incubating GC cells in the culture medium containing lentiviral particles for 12 h in the presence of 5 μ g ml⁻¹ Polybrene (Santa Cruz Biotechnology). Pooled puromycin (2 μ g ml⁻¹)-resistant cells were used for further analysis.

Stable transfection in GC cell lines. Control plasmid pcDNA3 and expression plasmids containing either human FOXO1A3 mutant gene (Addgene plasmid 13508) or HER2 wild-type (WT) gene (Addgene plasmid 16257) were purchased from Addgene Incorp. The plasmid FOXO1A3 encodes a constitutively active FOXO1 containing a threonine-to-alanine substitution at residue 24 and serine-to-alanine substitution at 256 and 319 (three AKT phosphorylation sites on FOXO1). Expression plasmid (1 μ g) or empty pcDNA3 vector (1 μ g) was transfected into 3×10^5 cells per well in six-well plates using Lipofectamine Plus according to the manufacturer's instructions. Pooled G418 (3 μ g ml⁻¹)-resistant cells were used for further analyses, as described previously (Park *et al*, 2014).

Colony formation assay. SNU-638 cells (2.5×10^3) expressing control shRNA or FOXO1 shRNA in 0.3% Bacto Agar (Sigma) in the RPMI 1640 medium with 10% FBS were overlaid onto a previously prepared 0.6% Bacto Agar in 12-well culture plates (Thermo Scientific, Rockford, IL, USA). The agar plates were incubated with 1 ml medium, which was changed every 3 days. After 15 days of culture, surviving colonies were stained with 0.05% crystal violet (Sigma) in 2% methanol. The number and size of colonies were determined using NIH Image Analysis software (version 1.46r; National Institutes of Health, Bethesda, MD, USA) as described previously (Takamaru *et al*, 2012).

Mouse xenograft model. All animal procedures were performed in accordance with the procedures described in the Seoul National University Laboratory Animal Maintenance Manual (approval no. SNU-140702-1). Six-week-old male nude mice (*BALB/cSlc-n/n*) were purchased from SLC Inc. (Hamamatsu, Shizuoka, Japan) and maintained under specific pathogen-free conditions.

For s.c. implantation, tumours were established by injecting SNU-638 GC cells expressing either control shRNA or FOXO1 shRNA at the density of 5×10^6 cells in 100 μ l of Matrigel (R&D Systems, Minneapolis, MN, USA) subcutaneously into the left flank of each mouse. Mice were divided into two groups by FOXO1 expression in GC cells: control shRNA or FOXO1 shRNA. Tumour volumes were measured every 2 days using a caliper, and were calculated by the equation $V \text{ (mm}^3\text{)} = (\text{length} \times \text{width} \times \text{height}) \times (\pi/6)$. Animals were killed 48 days after cell implantation, and tumour xenografts were removed.

For orthotopic implantation, animals were anaesthetised with a mask using 1.5% isoflurane. Then, after making a small median abdominal incision in the mice under anaesthesia, 5×10^6 GC cells (SNU-638, MKN45 and NCI-N87) in 50 μ l of Matrigel were inoculated into the submucosa of the stomach at the middle wall of the greater curvature using a 31-gauge needle. The stomach was then returned into the peritoneal cavity, and the abdominal wall and skin were closed (Yanagihara *et al*, 2005). Sixty days after transplantation or when moribund, the animals were killed and an autopsy was performed. The perpendicular diameters of the primary tumours were measured with calipers, and the volumes were calculated using the following formula: volume = length \times width \times (depth/2) (Hotz *et al*, 2012). Stomach and other metastasis-prone organs were removed, and processed for histological examination.

Immunofluorescence staining. SNU-638 GC cells were cultured on four-well chamber slide (Thermo Scientific). After 24 h, cells were fixed with 4% paraformaldehyde for 10 min, and blocked with 5% normal serum with 0.5% Triton X-100 for 5 min. Cells were incubated with a primary antibody against FOXO1 (1:200), E-cadherin (1:200) or Snail (1:200). Alexa Fluor-555-conjugated anti-rabbit IgG (1:200) or -488-conjugated anti-mouse IgG (1:200) was used as a secondary antibody. Then, cells were stained with DAPI (1 μ g ml⁻¹) for nuclear visualisation.

To examine whether FOXO1 silencing reorganises cytoskeleton, filamentous actin (F-actin) was visualised. Cells were incubated with 165 nM Alexa Fluor 633-conjugated phalloidin for 10 min, followed by DAPI staining. Immunofluorescence was observed under a fluorescence microscope as described previously (Yoon *et al*, 2013).

Transwell migration assay. A 24-well Insert System with an 8- μ m pore size polyethylene terephthalate membrane was purchased from BD Biosciences. Ten per cent FBS-containing medium was placed in the lower chambers to be used as a chemoattractant. Gastric cancer cells (1×10^4 cells per insert) in 300 μ l volume of 1% FBS-containing medium were seeded per Transwell and allowed to migrate for 48 h at 37 °C. Non-migrated cells were removed from the top of each insert with a cotton swab. Migrated cells on the bottom surface of the insert were stained with 0.2% crystal violet in 20% methanol for 30 min and were photographed with an inverted microscope. Stained cells were lysed with 10% SDS for 30 min, and absorbance was measured at 570 nm using an ELISA reader (Bio-Rad, Hercules, CA, USA) as described previously (Yoon *et al*, 2013).

Cell invasion assay. A 24-well Insert System described above was used. Transwell inserts were coated with Matrigel, followed by rehydration with medium for 2 h. Ten per cent FBS-containing medium was placed in the lower chambers to be used as a chemoattractant. Medium in the upper chambers was replaced by

1×10^5 GC cells in 300 μ l volume of 1% FBS-containing medium. After incubation for 48 h at 37 °C, non-invasive cells were removed with a cotton swab. Invasive cells on the lower surface of the insert were stained, photographed and lysed, followed by measuring absorbance as described above.

Assessment of cell growth. SNU-216 and NCI-N87 cells (2.5×10^4 cells per well) were seeded into 24-well plates and were allowed to grow for 0–72 h. Cell numbers were measured indirectly using the method reported by Kim *et al* (1994). Briefly, cells were stained with 0.2% crystal violet aqueous solution in 20% methanol for 10 min, dissolved in 10% SDS, transferred into 96-well plates and the absorbance was measured at 570 nm using an ELISA reader.

Patients and tissue array methods. Two hundred and forty-two surgically resected human GC specimens were obtained from the Department of Pathology, Seoul National University College of Medicine from 1 January to 30 June 1995. Five paraffin tissue array blocks were prepared as previously described (Lee *et al*, 2003). This protocol was reviewed and approved by the Institutional Review Board of the Seoul National University (approval no. C-1006-035-320).

Tumour histology and immunohistochemistry. Tissue specimens from clinical gastric carcinoma samples and xenograft tumours derived from GC cells were fixed with 10% neutral-buffered formalin and 4- μ m paraffin sections were then prepared. After rehydration, sections were stained with haematoxylin and eosin for histologic assessment, or were immunostained after antigen retrieval using a Bond-max automated immunostainer (Leica Microsystems, Newcastle, UK). The primary antibodies used were against HER2 (1:100), pFOXO1 (1:60) and FOXO1 (1:40). Antibody binding was detected with the Bond Polymer Refine Detection kit (Leica Microsystems). All immunostained sections were then lightly counterstained with Mayer's haematoxylin. Throughout the above analysis, negative controls were prepared by omitting the primary antibody.

For tissue array analysis of human GC specimens, HER2 immunostaining in cancer cells was scored in accordance with the HER2 scoring system for GC as described in a previous study (Kim *et al*, 2011). Briefly, cases showing weak to strong staining of the entire or basolateral membrane in $\geq 10\%$ of the tumour cells were considered HER2 immuno-positive. For the analysis of FOXO1 staining, cases showing cytoplasmic expression of pFOXO1 (inactive form of FOXO1) in $\geq 10\%$ of the tumour cells were considered pFOXO1 immuno-positive (Kim *et al*, 2007).

Semi-quantitative reverse transcription-PCR. To quantify mRNA levels of HER2, we used a highly sensitive semi-quantitative reverse transcription-PCR (SQ RT-PCR) method, as previously described (Chun *et al*, 2001). Total RNAs were isolated using TRIzol (Invitrogen) and 1 μ g RNA was reverse-transcribed at 48 °C for 30 min. Complementary DNAs were amplified over 20 PCR cycles (denaturation at 94 °C for 30 s, annealing at 52 °C for 30 s and extension at 70 °C for 30 s) in a reaction mixture containing 5 μ l (α -32 P)dCTP (NEN, Boston, MA, USA). The resulting PCR fragments (5 μ l) were electrophoresed on a 2% agarose gel at 100 V in 1 \times TAE, and the gels were dried and autoradiographed. Primer sequences were 5'-GGGAGAGAGTTCTGAGGATT-3' and 5'-CGT CCGTAGAAAGGTAGTTG-3' for HER2; and 5'-ACACCTTCTA CAATGAGCTG-3' and 5'-CATGATGGAGTTGAAGGTAG-3' for β -actin.

Chromatin immunoprecipitation. Chromatins were cross-linked with 1% formaldehyde for 10 min, followed by washing with ice-cold PBS. The cells were collected by scraping and centrifugation, and the pellets were lysed in the chromatin immunoprecipitation (ChIP) lysis buffer (50 mM HEPES, pH 7.5,

140 mM NaCl, 1 mM EDTA, 1% Triton X-100, 0.1% sodium deoxycholate, 0.1% SDS and a protease inhibitor cocktail). The lysates were sonicated to chop chromosomal DNAs into 400–700 bp pieces. The lysates were spun down and diluted by five-folds in a chromatin RIPA buffer (50 mM Tris, pH 8.0, 150 mM NaCl, 2 mM EDTA, 1% NP-40, 0.5% sodium deoxycholate, 0.1% SDS and a protease inhibitor cocktail). The samples were pre-cleaned with protein A/G beads, and 1% of each sample was used as the input control. The samples were immunoprecipitated with anti-FOXO1 or control IgG. The complex was washed with a buffer (20 mM Tris, pH 8.0, 0.1% SDS, 1% Triton X-100, 2 mM EDTA and 150 mM NaCl) and eluted with an elution buffer (1% SDS, 100 mM NaHCO₃). Immunoprecipitated DNAs were subjected to PCR amplification using specific primers. Quantitative real-time PCR was performed in the EvaGreen qPCR Mastermix (Applied Biological Materials Inc., Richmond, BC, Canada), and fluorescence emitting from dye-DNA complex was monitored in CFX Connect Real-Time Cycler (Bio-Rad). The quantitative real-time PCR primer sequences for HER2 were 5'-GATTCTCCGAGG AAAAGTGT-3' and 5'-AACTGCATTCCAACAAGTCT-3' for PM1; and 5'-TTTAGCAGACAGGGTTTC-3' and 5'-TCCTA GGGAGTTGAGAAACA-3' for PM2.

Statistical analysis. For cell culture and animal experiments, data were analysed using GraphPad Prism software for Windows 7 (version 4; GraphPad Software, San Diego, CA, USA) and the two-tailed Student's *t*-test was used to determine the significances of the results. For tissue array analysis, statistical analyses were conducted using SPSS version 19.0 statistical software programme (IBM SPSS, Chicago, IL, USA), and the χ^2 -test was used to determine the relationship between the expressions of pFOXO1 and HER2. Results are expressed as mean \pm s.d. $P < 0.05$ was considered statistically significant.

RESULTS

FOXO1 expression is inversely associated with GC cell growth *in vitro* and *in vivo*. To investigate the role of FOXO1 in the tumour growth of GC, we modulated FOXO1 expression in GC cells. Figure 1A shows the varying protein contents of FOXO1 in four GC cell lines. SNU-216 and SNU-484 showed low levels of FOXO1 expression and activity, whereas SNU-638 and MKN45 showed high levels. We selected SNU-638 and MKN45 cell lines and produced stable cell lines infected with lentiviral particles containing non-targeting (control) or FOXO1-targeting shRNA. Immunoblot analysis confirmed the downregulation of FOXO1 expression in both cell lines expressing FOXO1 shRNA (Figure 1B).

To examine the role of FOXO1 in GC cell growth, soft-agar colony formation assay was performed using cultured SNU-638 GC cells. We found that FOXO1 silencing enhanced the colony formation (Figure 1C). Then, growth inhibitory activity of FOXO1 in GC was further confirmed using a s.c. xenograft mouse model (Figure 1D). We injected SNU-638 cells stably expressing control shRNA or FOXO1 shRNA subcutaneously into nude mice, and found that xenograft tumours were successfully formed in all mice (Figure 1D, left). Forty-eight days after injection, the average volume of FOXO1 shRNA tumours was 342.7 mm³ (ranged from 239.5 to 461.6 mm³) compared with 103.8 mm³ (ranged from 59.8 to 157.9 mm³) of control shRNA tumours (Figure 1D, right). Thus, the tumour volume was markedly increased in mice injected with FOXO1 shRNA-expressing cells compared with those injected with control shRNA-expressing cells ($P = 0.025$). However, as previously reported by Sekikawa *et al* (1988), none of the mice showed tumour metastasis.

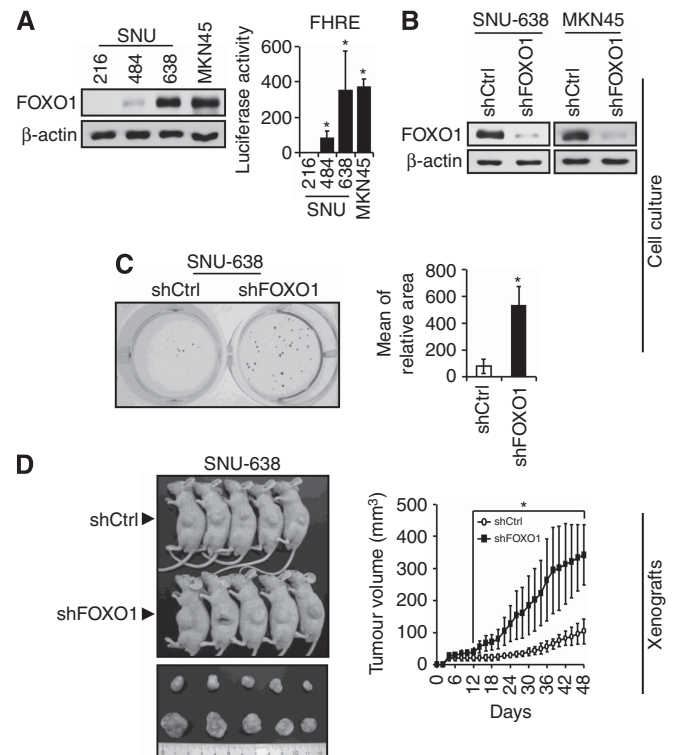


Figure 1. Effect of FOXO1 expression on GC cell growth *in vitro* and *in vivo*. (A) Protein expression and activation of FOXO1 in human GC cell lines were determined by immunoblot analysis and luciferase reporter assay. Bars represent mean \pm s.d. ($n = 4$). * $P < 0.05$, compared with SNU-216 cells. (B) GC cell lines (SNU-638 and MKN45) with high levels of FOXO1 expression and activity were infected with a lentivirus containing a construct, which encodes either control shRNA (denoted as shCtrl) or FOXO1 shRNA (denoted as shFOXO1). FOXO1 protein expression was determined by immunoblot analysis. (C) Soft-agar colony formation assay. Anchorage-independent growth of SNU-638 cells expressing shCtrl or shFOXO1 was measured in soft agar. On day 15 after plating, quantification of colony formation was performed by setting the number and size of colonies derived from shCtrl-expressing cells as 100%. Bars represent mean \pm s.d. ($n = 3$). * $P < 0.05$, compared with shCtrl. (D) SNU-638 cells expressing shCtrl or shFOXO1 were injected subcutaneously into the left flanks of BALB/c nude mice ($n = 5$ per group). Representative photos of mice taken after killing at day 48 are displayed (left). The size of the tumour was measured over time (right). * $P < 0.05$, compared with shCtrl.

FOXO1 expression negatively regulates EMT, migration and invasion of GC cells. In the initial steps of metastasis of carcinoma cells, epithelial cancer cells change their phenotype to a mesenchymal phenotype by a process called epithelial-mesenchymal transition (EMT) (Nurwidya *et al*, 2012). Thus, we investigated the effect of FOXO1 on EMT in SNU-638, MKN45 and SNU-216 GC cells. Immunoblot analysis (Figure 2A and E) and immunofluorescence staining (Figure 2C) showed that FOXO1 shRNA expression decreased E-cadherin (an epithelial marker) expression, but increased Snail (a mesenchymal marker) expression in SNU-638 and MKN45 cells, which suggested the inhibitory role of FOXO1 in the context of mesenchymal transition. To further confirm these results, we examined actin organisation because actin-dependent membrane protrusions act as critical determinants of EMT (Shankar *et al*, 2010). Staining of filamentous actin with FITC-conjugated phalloidin revealed the presence of many filopodia-like extensions containing actin-rich bundles in the FOXO1 shRNA-expressing cells. However, they

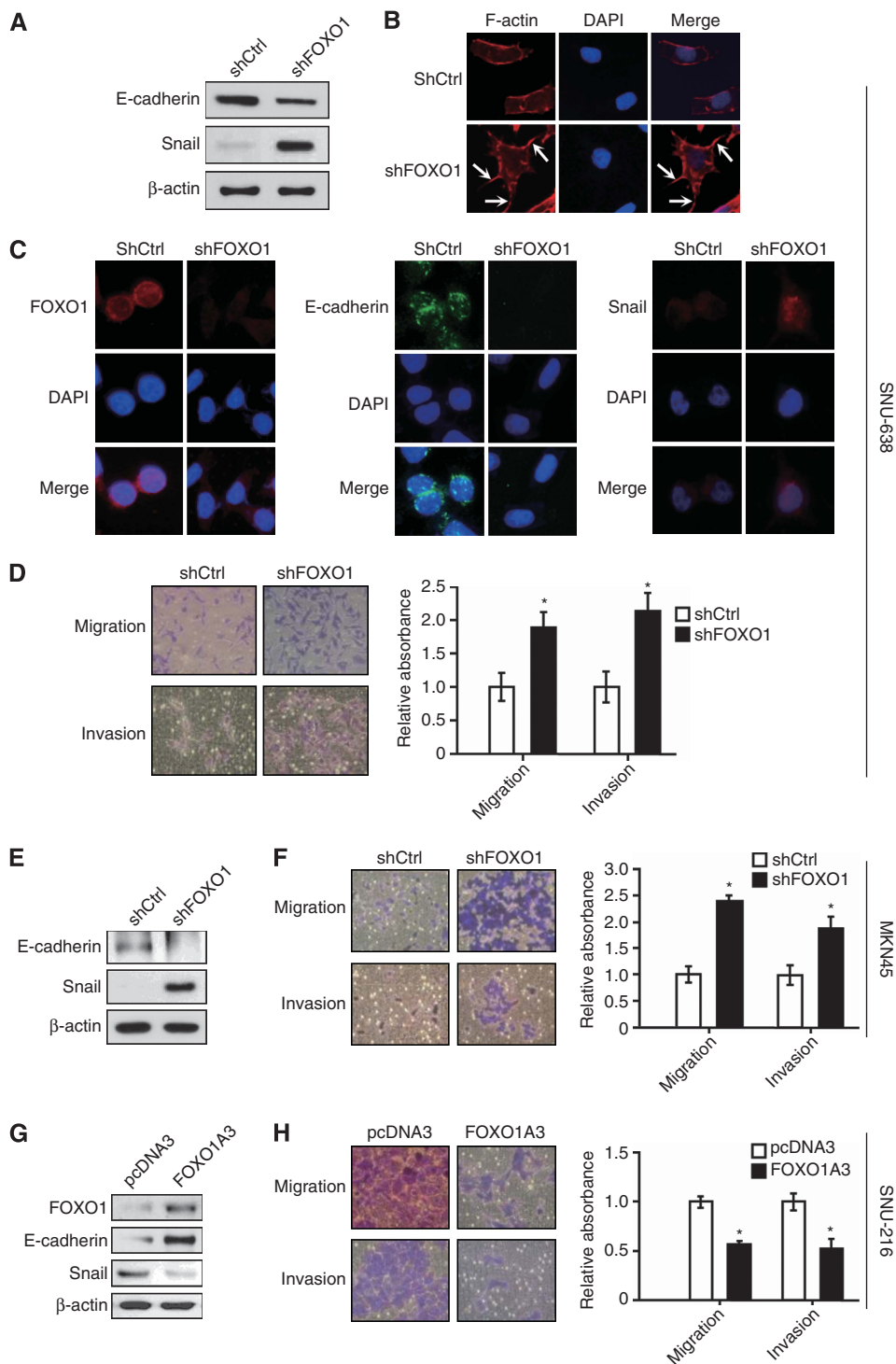


Figure 2. The *in vitro* effect of FOXO1 on EMT, cell migration and invasion of SNU-638 cells, MKN45 cells and SNU-216 cells. **(A and E)** The expressions of E-cadherin and Snail in GC cells expressing either control shRNA (shCtrl) or FOXO1 shRNA (shFOXO1) were determined by immunoblot analysis. **(B)** Changes in the organisation of the actin cytoskeleton. Cells were stained with Alexa Fluor 633-conjugated phalloidin to visualise F-actin (red), and the cell nuclei were visualised by DAPI staining (blue). Arrows indicate the FITC-labelled filopodia-like projections. Photographs were taken with a fluorescence microscope ($\times 400$ magnification). **(C)** Immunofluorescence stainings for FOXO1 (red), E-cadherin (green) and Snail (red) were performed. Cell nuclei were visualised by DAPI staining (blue) ($\times 400$ magnification). **(D and F)** The effect of FOXO1 silencing on cell migration/invasion was evaluated by Transwell migration assay and cell invasion assay followed by cell viability assessment using the crystal violet assay. Representative images of migrated/invasive cells taken 48 h after plating into a Transwell insert are on the left, and the quantification of migrated/invasive cells is on the right. The motility/invasiveness of cells expressing shCtrl corresponded to 1. Bars represent mean \pm s.d. ($n = 4$). $*P < 0.05$, compared with shCtrl. **(G and H)** SNU-216 cells were transfected with either control plasmid pcDNA3 or pFOXO1A3 (FOXO1A3). **(G)** The effect of FOXO1A3 transfection into GC cells on the expression of E-cadherin and Snail was determined by immunoblot analysis. **(H)** The effect of FOXO1A3 expression in GC cells on the cell migration and invasion was determined as described above. Bars represent mean \pm s.d. ($n = 4$). $*P < 0.05$, compared with vector control (pcDNA3).

were absent or less obvious in the control shRNA-expressing cells (Figure 2B).

We next examined the effect of FOXO1 knockdown on the migration and invasion of these cell lines. Our data showed that FOXO1 shRNA-expressing GC cells (SNU-638 and MKN45) showed significantly increased migration ($P = 0.001$ and $P = 0.005$, respectively) and invasion ($P < 0.001$ in both cell lines) compared with their respective controls (Figure 2D and F). Thus, it seems that FOXO1 is inversely associated with EMT and metastatic potential.

In addition, we transfected a FOXO1A3 mutant gene into SNU-216 GC cells with low levels of FOXO1 expression and activity. FOXO1 upregulation increased E-cadherin expression, but decreased Snail expression (Figure 2G), as well as cell migration and invasion (Figure 2H). Thus, FOXO1 expression reverses EMT and suppresses metastatic potential in GC cells.

FOXO1 silencing enhances orthotopic GC growth and metastasis.

Since s.c. GC xenograft was not suitable for inducing GC metastasis, we established an orthotopic GC xenograft model

according to a previous report (Yanagihara *et al*, 2005). Figure 3 shows the summary of the tumour incidence and site of metastasis (Figure 3A) and representative macroscopic (Figure 3B–E) and microscopic (Figure 3F) pictures. Sixty days after the implantation of SNU-638 cells expressing control shRNA or FOXO1 shRNA, four out of five (80%) mice injected with FOXO1 shRNA transfectants had primary tumours in the stomach and/or metastatic tumours in the veins, lymph nodes, liver, pancreas and oesophagus. However, none of the mice implanted with control shRNA transfectants had primary or metastatic tumours.

When MKN45 cells expressing control shRNA or FOXO1 shRNA were injected, the same incidence of primary tumour formation (11 of 15) was shown in both groups of mice (Figure 3A) although FOXO1 shRNA tumours were larger than the control shRNA tumours (Figure 3C). The average volume of FOXO1 shRNA tumours was 232.5 mm^3 (range from 1.5 to 720.0 mm^3) compared with 106.2 mm^3 (range from 1.5 to 432.0 mm^3) of control shRNA tumours. Although macroscopic and histologic examinations showed that both groups of tumours showed venous

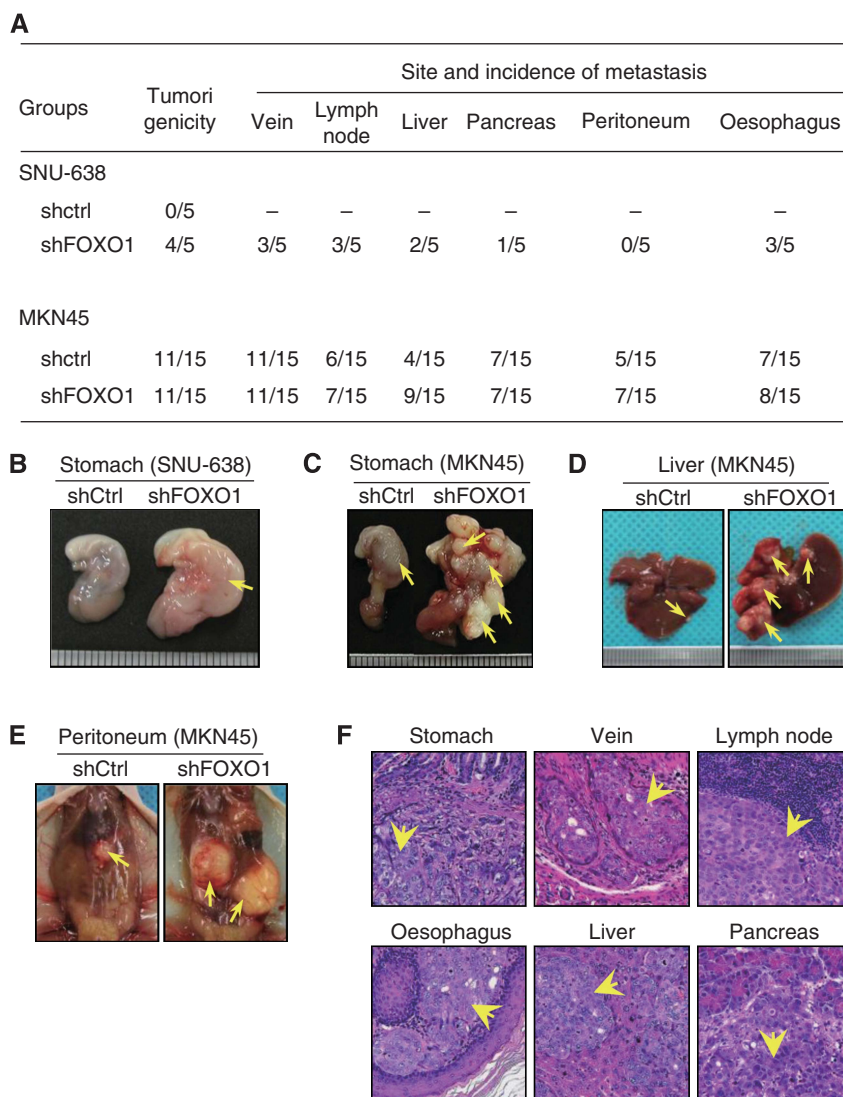


Figure 3. Effects of FOXO1 silencing on orthotopic tumour formation and metastasis in a mice model. GC cells (SNU-638 and MKN45) expressing control shRNA (shCtrl) or FOXO1 shRNA (shFOXO1) were orthotopically xenografted into the stomach (submucosa) and were grown for 60 days. (A) Numbers of mice showing primary tumour formation, as well as site and incidence of metastasis are shown. (B–E) Representative photographs showing the macroscopic appearances of the stomach (B and C), liver (D) and peritoneum (E) from animals implanted with either shCtrl transfectants (left) or shFOXO1 transfectants (right). (F) Histological appearance of organs showing primary (stomach) or metastatic (vein, lymph node, oesophagus, liver and pancreas) tumours. Arrows indicate primary or metastatic foci ($\times 200$ magnification).

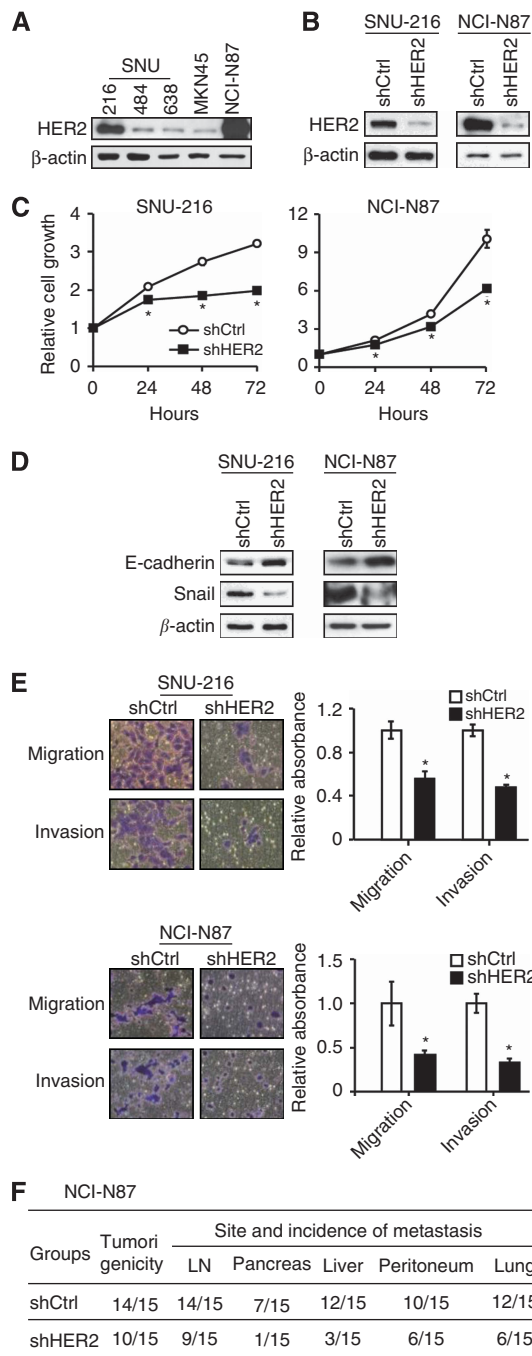


Figure 4. Effects of HER2 silencing on oncogenic behaviours of GC cell lines *in vitro* and *in vivo*. (A) Expression of HER2 protein in parent GC cell lines was determined by immunoblot analysis. (B) GC cell lines (SNU-216 and NCI-N87) expressing a high level of HER2 were infected with a lentivirus containing either control shRNA (shCtrl) or HER2 shRNA (shHER2). HER2 protein expression was determined by immunoblot analysis. (C) Cells were cultured for 0–72 h and cell growth was determined using the crystal violet assay at the indicated times. The data are presented as mean \pm s.d. ($n = 6$). * $P < 0.05$, compared with shCtrl. (D) The effect of shHER2 transfection on the expressions of E-cadherin and Snail was determined by immunoblot analysis. (E) Effects of shHER2 transfection on cell migration and invasion of GC cells were analysed by Transwell migration assay and invasion assay, respectively. Bars represent mean \pm s.d. ($n = 4$). * $P < 0.05$, compared with shCtrl. (F) NCI-N87 cells expressing shCtrl or shHER2 were orthotopically injected into the stomach and were grown for 60 days ($n = 15$ per group). The numbers of mice showing primary tumour formation, as well as site and incidence of metastasis are shown.

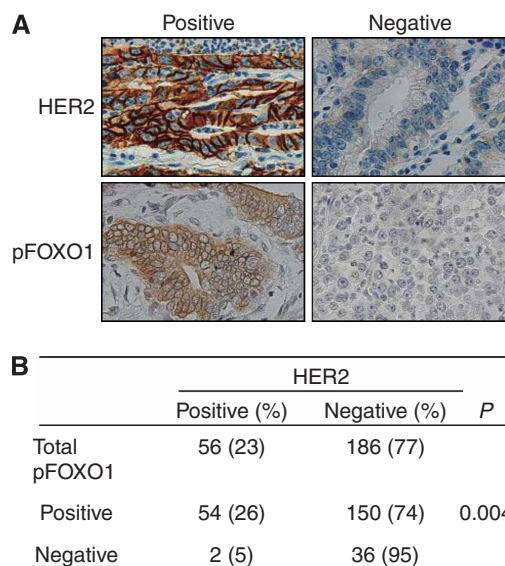


Figure 5. Representative immunohistochemical features of HER2 and pFOXO1 in human GC specimens. (A) Positive versus negative examples for HER2 and pFOXO1 ($\times 400$ magnification). (B) Statistical analysis was performed using χ^2 -test. A positive relationship between the expressions of membranous HER2 and cytoplasmic pFOXO1 are shown ($P = 0.004$).

invasion and metastases to various organs (Figure 3D–F), liver metastasis increased to 82% (9 out of 11) in FOXO1 shRNA-expressing MKN45 tumours compared with 36% (4 out of 11) in control shRNA-expressing MKN45 tumours.

HER2 downregulation inhibits tumour cell growth, EMT, cell migration and invasion, tumorigenicity and metastasis of GC. Previously, HER2 downregulation was shown to decrease GC cell migration and invasion *in vitro* (Bao *et al.*, 2010) and tumour growth *in vivo* (Bao *et al.*, 2011). We used RNA interference to downregulate HER2 expression to confirm the oncogenic effect of HER2 in GC cell lines used in the present study. Since HER2 protein expression in GC cell lines varied (Figure 4A), we selected SNU-216 and NCI-N87 GC cell lines showing a high level of HER2 expression. Permanent transfection of HER2 shRNA into these cell lines downregulated HER2 expression (Figure 4B) and decreased cell growth (Figure 4C) compared with non-targeting shRNA transfection. Furthermore, E-cadherin increased and Snail decreased in HER2 shRNA-expressing GC cells compared with the control shRNA-expressing GC cells (Figure 4D), indicating the stimulatory role of HER2 in the EMT of GC cells. Consistently, HER2 silencing decreased the cell migration and invasion of GC cells (Figure 4E). Although we tried to examine the effect of HER2 silencing on GC cell metastasis *in vivo*, SNU-216 cells did not show tumorigenesis after orthotopic implantation. Thus, we established orthotopic GC xenografts by injecting NCI-N87 cells expressing either control shRNA or HER2 shRNA. Our results showed that, for the first time, HER2 shRNA expression in GC cells decreased the incidence of metastatic tumours in the lymph nodes, pancreas, liver, peritoneum and the lungs compared with the control shRNA (Figure 4F).

An inverse relationship between HER2 and FOXO1 exists in clinical specimens of GC. To investigate the association between HER2 and FOXO1 in human GC, immunohistochemical tissue array analysis of 242 human GC specimens was performed. Cancer cells with membranous HER2 expression were considered to exhibit HER2 activation (Figure 5A, upper), and those with cytoplasmic staining of pFOXO1, regardless of nuclear staining, were considered to exhibit FOXO1 inactivation (Figure 5A, lower).

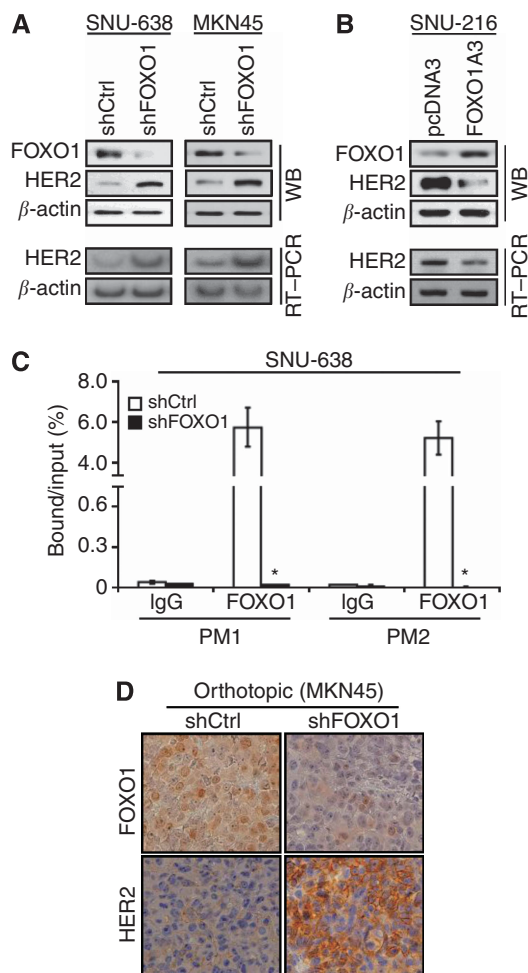


Figure 6. Effects of FOXO1 silencing on HER2 expression in GC cells and xenograft tumours. **(A)** FOXO1 was downregulated by transfection of FOXO1 shRNA (shFOXO1) into SNU-638 and MKN45 cells. Immunoblot analysis (WB) and RT-PCR showed that FOXO1 shRNA transfection increased the expressions of HER2 protein and mRNA compared with control shRNA (shCtrl) transfection. **(B)** FOXO1 expression in SNU-216 cells was upregulated by transfection of FOXO1A3. WB and RT-PCR showed that FOXO1A3 transfection decreased HER2 protein and mRNA expressions compared with pcDNA3 transfection. **(C)** CHIP for the binding of FOXO1 to the HER2 promoter in SNU-638 cells. Chromatin was cross-linked and immunoprecipitated using anti-FOXO1. Precipitated DNAs were amplified and quantified by real-time PCR using two primers (PM1 and PM2). The results are expressed as percentages of the input level. Bars represent mean \pm s.d. ($n = 3$). * $P < 0.05$, compared with shCtrl. **(D)** Representative features of immunohistochemical staining for FOXO1 (upper panels) and HER2 (lower panels). Sections obtained from orthotopic xenograft tumours showed that shFOXO1-expressing tumours had higher HER2 expression than shCtrl-expressing tumours ($\times 400$ magnification).

Figure 5B shows that membranous HER2 activation is positively correlated with FOXO1 inactivation ($P = 0.004$), indicating an inverse association between the activation of these two molecules.

Crosstalk between FOXO1 and HER2 exists in GC cells. To confirm this relationship, cell culture and animal experiments were performed. Immunoblot analysis of cultured cells (Figures 1A and 4A) showed that SNU-638 and MKN45 cells with a high level of FOXO1 expression showed a low level of HER2 expression, whereas SNU-216 and NCI-N87 cells with a low level of FOXO1

expression showed a high level of HER2 expression. Furthermore, FOXO1 silencing in SNU-638 and MKN45 cells by RNA interference increased the expressions of HER2 protein and mRNA (Figure 6A), whereas FOXO1 overexpression in SNU-216 cells by transfection of FOXO1A3 induced the opposite results (Figure 6B). Thus, these results indicate that FOXO1 is a negative regulator of HER2 expression at the transcriptional level in GC cells.

We subsequently investigated if FOXO1 regulates HER2 expression directly through the binding of specific sites within the HER2 promoter. Chromatin immunoprecipitation analyses followed by quantitative real-time PCR using two primers showed that FOXO1 shRNA transfection markedly reduced the binding of FOXO1 to HER2 promoter to a negligible level ($P < 0.001$) (Figure 6C). Consistently, immunohistochemical analysis of orthotopic xenografts derived from MKN45 cells showed that FOXO1 shRNA expression increased membranous HER2 expression in GC cells (Figure 6D).

To investigate the role of HER2 on FOXO1 activation in GC cells, we used SNU-216 and NCI-N87 cells expressing control shRNA or HER2 shRNA. We found that HER2 knockdown increased FOXO1 expression and activation in both cell lines (Figure 7A). Consistently, xenograft tumours derived from NCI-N87 showed increased FOXO1 expression in the nuclei of GC cells (Figure 7B).

To verify the involvement of the PI3K/AKT pathway in HER2-induced FOXO1 inhibition, SNU-638 and MKN45 cells were transfected with a control plasmid (pcDNA3) or HER2 WT plasmid (HER2-WT), and were treated with a PI3K inhibitor LY294002 or an AKT inhibitor IV (Figure 7C). Immunoblot analysis showed that HER2 overexpression increased the expressions of the active form of AKT (pAKT) and its substrate GSK-3 β (pGSK-3 β), which was subsequently suppressed by treatment with LY294002 or AKT inhibitor IV (Figure 7C, left). In the luciferase reporter assay, HER2 overexpression inhibited the activity of FOXO1, but subsequent AKT inhibition effectively restored the activity of FOXO1 (Figure 7C, right). These results indicate that HER2 inhibits the activity of FOXO1 through the activation of the PI3K/AKT signalling.

Double knockdown of both FOXO1 and HER2 nearly cancels the effect of FOXO1 silencing on cell migration and invasion. The aforementioned results showed that the metastatic capacity of GC cells was decreased by FOXO1 and increased by HER2. Thus, we wondered which one of these molecules was more important to the metastatic potential of GC cells. We found that single transfection of FOXO1 shRNA into GC cells increased HER2 expression (Figure 8A), as well as cell migration and invasion (Figure 8B and C), which were completely suppressed by HER2 shRNA overexpression in spite of the lack of the restoration of FOXO1.

DISCUSSION

The biological significance of FOXO1 activation could be cancer cell-type specific, but there is little information on the role and the underlying molecular mechanisms of FOXO1 activation in GC. To the best of our knowledge, the present study is the first to provide direct evidence on the role of FOXO1 in GC growth and metastasis through the regulation of HER2 expression.

Although metastasis mainly determines the poor outcome of GC patients, the molecular mechanisms underlying GC metastasis remain unclear. Since tumour growth is critical to the metastasis of cancer cells, we first investigated the effect of FOXO1 on GC cell growth *in vitro* and *in vivo*. Our results showed that FOXO1 silencing by RNA interference increased colony formation, and tumour growth of s.c. and orthotopic xenografts.

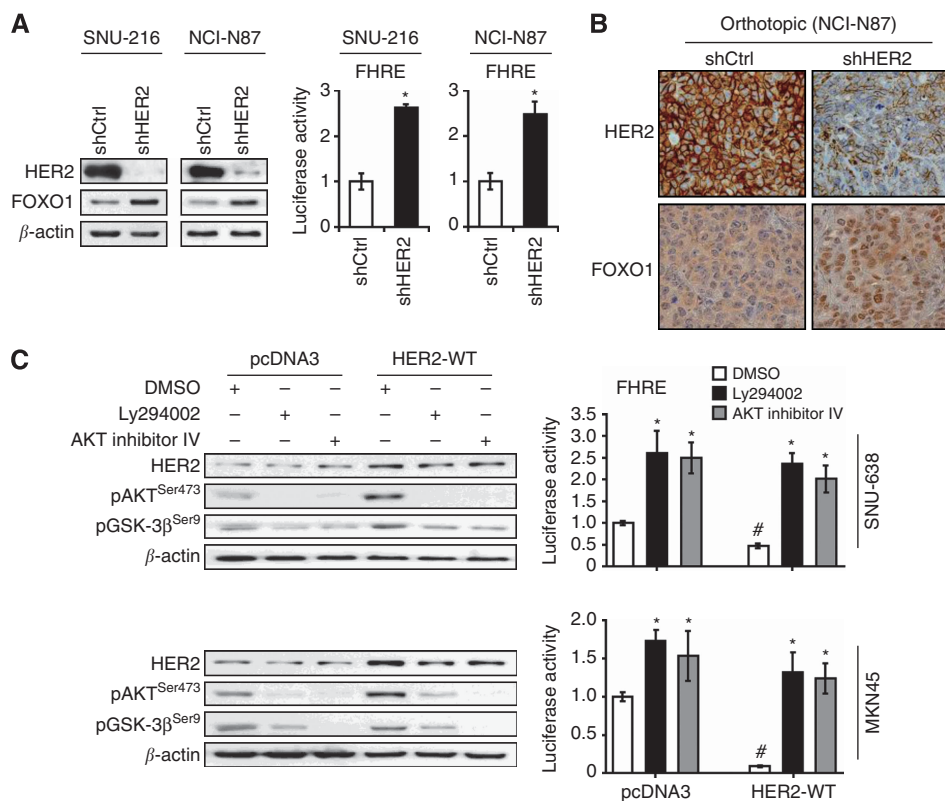


Figure 7. Effects of HER2 modulation on FOXO1 activation through PI3K/AKT pathway in GC cells and xenograft tumours. **(A)** SNU-216 and NCI-N87 cells were incubated with lentiviral particles containing a control shRNA (shCtrl) or HER2 shRNA (shHER2). The effects of HER2 silencing on FOXO1 expression and activation were determined by immunoblot analysis (left) and luciferase reporter assay (right), respectively. Luciferase activity in shCtrl cells was arbitrarily set to 1. Bars represent mean \pm s.d. ($n=4$). * $P<0.05$, compared with shCtrl. **(B)** Representative features of immunohistochemical staining for HER2 (upper panels) and FOXO1 (lower panels). Sections obtained from orthotopic xenograft tumours showed that shHER2-expressing tumours had higher FOXO1 expression in the nuclei of cancer cells than shCtrl-expressing tumours ($\times 400$ magnification). **(C)** SNU-638 and MKN45 cells were transfected with either a control plasmid pcDNA3 (pcDNA3) or an expression plasmid containing HER2 wild-type gene (HER2-WT). Cells were treated with a PI3K inhibitor LY294002 ($30\ \mu\text{M}$) or an AKT inhibitor IV ($0.5\ \mu\text{M}$) for 24 h, and immunoblot analysis was performed using the antibodies indicated in the figure (left). Luciferase reporter assay for FOXO1 transcriptional activity was also performed (right). Bars represent mean \pm s.d. ($n=4$). * $P<0.05$, compared with vehicle control (DMSO). # $P<0.05$, compared with vector control (pcDNA3).

Furthermore, analysis of the metastatic potential of FOXO1 showed that FOXO1 downregulation induced mesenchymal phenotype and the increased migratory and invasive potential of GC cells. Thus, our data provide direct evidence for the role of FOXO1 as a tumour suppressor in GC cells via modulating oncogenic behaviours.

Tumour cell genotype and phenotype have generally been considered as the only determinants of cancer growth and metastasis, but cancer cell behaviour is also influenced by their microenvironment (Chung *et al*, 2005). Animal models of metastasis have identified metastasis suppressor and promoter genes as novel cancer therapy targets (Rosol *et al*, 2003). However, local invasive growth characteristics and metastatic potential can differ markedly between tumours at different inoculation sites (Sekikawa *et al*, 1988). Previously, the limitations of the s.c. xenograft tumours, including rapid growth, encapsulation and difficulty to metastasise, were reported (Sekikawa *et al*, 1988). Indeed, our study showed that s.c. GC xenografts were successfully derived from SNU-638 cells expressing either control shRNA or FOXO1 shRNA in 100% of the injected nude mice. However, they did not show metastasis to any of the organs of the mice. Thus, FOXO1 alteration in SNU-638 cells alone was not enough to confer metastatic status *in vivo* without an appropriate tumour microenvironment.

In the present study, we established orthotopic GC xenografts to observe the effect of FOXO1 on GC cell metastasis. When SNU-638 cells expressing control shRNA or FOXO1 shRNA

were injected into nude mice, primary tumours with or without metastatic foci were found in 80% (four of five) of mice inoculated with FOXO1 shRNA transfectants. In contrast, control shRNA transfectants did not induce any tumours. Thus, further experiments were performed using MKN45 cells expressing control shRNA or FOXO1 shRNA. Although both groups of mice showed the same incidence of primary tumour formation (11 of 15), tumours derived from the FOXO1 shRNA-transfected cells were larger and showed higher metastatic incidence in the liver. Thus, these results indicate that FOXO1 expression is directly associated with the suppression of gastric tumour growth and metastasis.

Earlier studies showed that HER2 knockdown decreased tumour growth of s.c. xenografts derived from GC cells (Bao *et al*, 2011), as well as GC cell migration and invasion *in vitro* (Bao *et al*, 2010). In the present study, we confirmed the effect of HER2 silencing on cell migration and invasion *in vitro* and GC growth *in vivo*. In addition, HER2 shRNA expression in GC cells markedly decreased the incidence of metastatic tumours in the lymph nodes, pancreas, liver, peritoneum and lungs compared with control shRNA. Thus, our orthotopic xenograft model, for the first time, clearly proved the direct effect of HER2 on GC metastasis. Taken together, these results indicate that FOXO1 and HER2 induce opposite effects on GC promotion.

Multiple signalling cascades converge at FOXO1 and the detailed molecular mechanisms underlying FOXO1 activation could be cancer cell-type specific (Feng *et al*, 2011). Since it

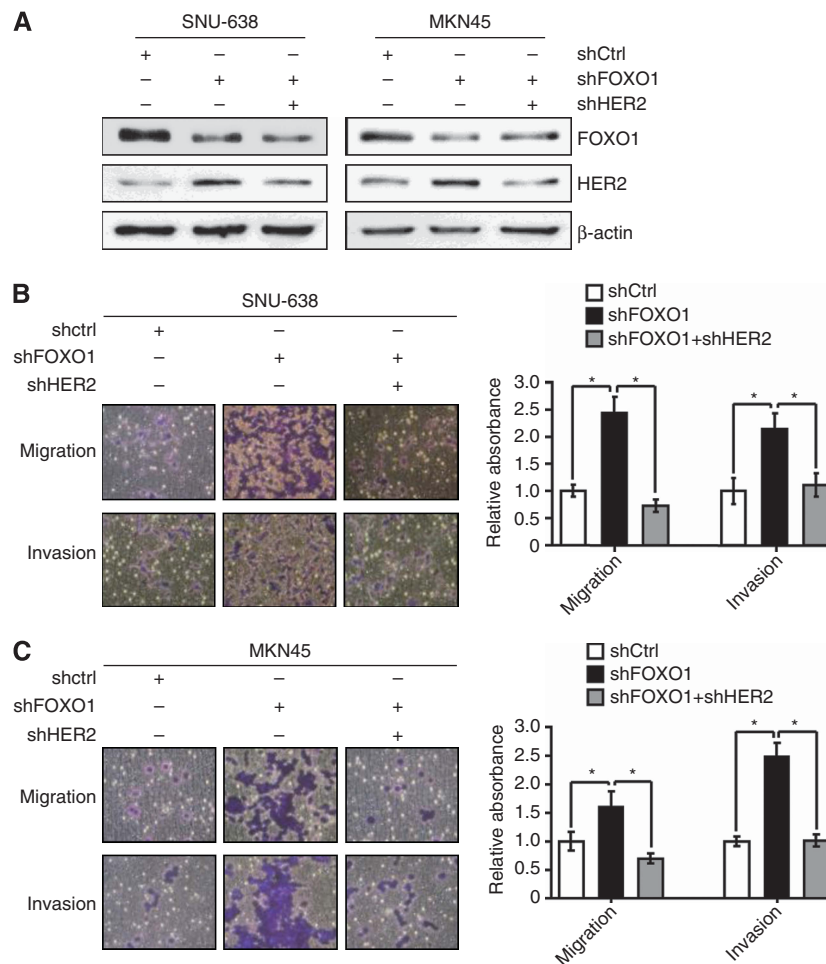


Figure 8. Effects of cotransfection of FOXO1 shRNA and HER2 shRNA on the cell migration and invasion of GC cell lines. **(A)** GC cell lines (SNU-638 and MKN45) were transfected with FOXO1 shRNA (shFOXO1), HER2 shRNA (shHER2) or both shRNAs. The protein expressions of FOXO1, HER2 and β -actin were determined by immunoblot analysis. **(B and C)** The effects of transfections of shFOXO1, shHER2 or both shRNAs on the cell migration and invasion were analysed 48 h after plating by Transwell migration assay and cell invasion assay. These data were quantified as described above. Bars represent mean \pm s.d. ($n=4$). * $P < 0.05$, compared with shFOXO1.

remains unknown whether a relationship between FOXO1 and HER2 exists in GC, we performed immunohistochemical tissue array analysis of 242 clinical GC specimens and found an inverse relationship between FOXO1 and HER2. Further *in vitro* analysis showed that FOXO1 silencing in SNU-638 and MKN45 cells increased HER2 expression at the transcriptional level, whereas FOXO1 overexpression in SNU-216 cells induced opposite results. Moreover, ChIP analysis revealed that FOXO1 directly interacted with the HER2 promoter, which suggested the competition of FOXO1 with other transcription factors for a binding site in the HER2 gene promoter.

In the present study, HER2 knockdown increased FOXO1 protein expression and activation in GC cells and orthotopic xenograft tumours, which indicates a negative reciprocal regulatory loop between FOXO1 and HER2 in GC. Previously, it was shown that treatment of HER2-amplified GC cell lines (SNU-216 and NCI-N87) with HER2 inhibitors decreased AKT activation (Nam *et al*, 2011; Kim *et al*, 2014). In addition, we found an inverse correlation between the activations of AKT and FOXO1 in human GC tissue specimens (Kim *et al*, 2007). In the present study, we examined whether PI3K/AKT signalling mediates HER2-induced FOXO1 inhibition and found that PI3K/AKT inhibition restored the activity of FOXO1, which was downregulated by HER2 overexpression. Thus, it seems that

HER2 inhibited the activity of FOXO1 in GC cells through PI3K/AKT signalling.

The present study showed that FOXO1 and HER2 induced opposite effects on the malignant phenotypes of GC cells *in vitro* and *in vivo*, and that FOXO1 was negatively controlled by and controls HER2. Thus, we compared the importance of these two molecules in the regulation of GC metastasis using cotransfection of FOXO1 shRNA and HER2 shRNA into SNU-638 and MKN45 cells. We found that HER2 expression and metastatic potential in GC cells were increased by FOXO1 shRNA transfection, but these changes were reversed after the subsequent transfection of HER2 shRNA in spite of the lack of the restoration of FOXO1. Thus, it appears that dysregulation of FOXO1 may increase GC growth and metastasis through the altered expression of HER2 and that HER2 expression, rather than FOXO1 expression, is more critical to the induction of GC cell metastasis. This speculation is supported by the more evident changes in the metastatic incidence induced by HER2 shRNA transfection than those induced by FOXO1 shRNA transfection.

In conclusion, the loss of FOXO1 in GC cells increased tumour growth and metastasis, whereas HER2 downregulation showed the opposite results. In addition, there was an inverse relationship between FOXO1 and HER2 in human GC specimens, GC cells and xenograft tumours in nude mice. Although the tumour-promoting

function of HER2 may be through diverse molecular mechanisms, the FOXO1/HER2 pathway may be useful in regulating GC growth and metastasis in a subgroup of GC patients. The present study provides important evidence that expands our current knowledge of the metastasis of GC.

ACKNOWLEDGEMENTS

This study was supported by Grant NO 04-2012-0240 from SNUH Research Fund, the National Research Foundation of Korea (NRF) Grant funded by the Korean Government (2010-0024702) and the Education and Research Encouragement Fund of Seoul National University Hospital. YSK was partly supported by the Korea Foundation for Cancer Research (KFCR-2010-004).

CONFLICT OF INTEREST

The authors declare no conflict of interest.

REFERENCES

- Bang YJ (2012) Advances in the management of HER2-positive advanced gastric and gastroesophageal junction cancer. *J Clin Gastroenterol* **46**: 637–648.
- Bao W, Fu HJ, Jia LT, Zhang Y, Li W, Jin BQ, Yao LB, Chen SY, Yang AG (2010) HER2-mediated upregulation of MMP-1 is involved in gastric cancer cell invasion. *Arch Biochem Biophys* **499**: 49–55.
- Bao W, Fu HJ, Xie QS, Wang L, Zhang R, Guo ZY, Zhao J, Meng YL, Ren XL, Wang T, Li Q, Jin BQ, Yao LB, Wang RA, Fan DM, Chen SY, Jia LT, Yang AG (2011) HER2 interacts with CD44 to up-regulate CXCR4 via epigenetic silencing of microRNA-139 in gastric cancer cells. *Gastroenterology* **141**: 2076–2087.
- Chen J, Huang Q, Wang F (2014) Inhibition of FoxO1 nuclear exclusion prevents metastasis of glioblastoma. *Tumour Biol* **35**: 7195–7200.
- Chun YS, Choi E, Yeo EJ, Lee JH, Kim MS, Park JW (2001) A new HIF-1 α variant induced by zinc ion suppresses HIF-1-mediated hypoxic responses. *J Cell Sci* **114**: 4051–4061.
- Chung LW, Baseman A, Assikis V, Zhou HE (2005) Molecular insights into prostate cancer progression: the missing link of tumor microenvironment. *J Urol* **173**: 10–20.
- Ding H, Zhu Y, Chu T, Wang S (2014) Epidermal growth factor induces FoxO1 nuclear exclusion to activate MMP7-mediated metastasis of larynx carcinoma. *Tumour Biol* **35**: 9987–9992.
- Feng X, Wu Z, Wu Y, Hankey W, Prior TW, Li L, Ganju RK, Shen R, Zou X (2011) Cdc25A regulates matrix metalloproteinase 1 through Foxo1 and mediates metastasis of breast cancer cells. *Mol Cell Biol* **31**: 3457–3471.
- Hotz B, Keilholz U, Fusi A, Buhr HJ, Hotz HG (2012) *In vitro* and *in vivo* antitumor activity of cetuximab in human gastric cancer cell lines in relation to epidermal growth factor receptor (EGFR) expression and mutational phenotype. *Gastric Cancer* **15**: 2522–2564.
- Kim HP, Han SW, Song SH, Jeong EG, Lee MY, Hwang D, Im SA, Bang YJ, Kim TY (2014) Testican-1-mediated epithelial-mesenchymal transition signaling confers acquired resistance to lapatinib in HER2-positive gastric cancer. *Oncogene* **33**: 3334–3341.
- Kim JH, Kim MK, Lee HE, Cho SJ, Cho YJ, Lee BL, Lee HS, Nam SY, Lee JS, Kim WH (2007) Constitutive phosphorylation of the FOXO1A transcription factor as a prognostic variable in gastric cancer. *Mod Pathol* **20**: 835–842.
- Kim MA, Lee HJ, Yang HK, Bang YJ, Kim WH (2011) Heterogeneous amplification of ERBB2 in primary lesions is responsible for the discordant ERBB2 status of primary and metastatic lesions in gastric carcinoma. *Histopathology* **59**: 822–831.
- Kim SY, Ko YS, Park J, Choi Y, Park JW, Kim Y, Pyo JS, Yoo YB, Lee JS, Lee BL (2015) Forkhead transcription factor FOXO1 inhibits angiogenesis in gastric cancer in relation to SIRT1. *Cancer Res Treat*; e-pub ahead of print 3 March 2015; doi:10.4143/crt.2014.247.
- Kim WH, Schnaper HW, Nomizu M, Yamada Y, Kleinman HK (1994) Apoptosis in human fibrosarcoma cells is induced by a multimeric synthetic Tyr-Ile-Gly-Ser-Arg (YIGSR)-containing polypeptide from laminin. *Cancer Res* **54**: 5005–5010.
- Lazrek Y, Dubreuil O, Garambois V, Gaborit N, Larbouret C, Le Cloennec C, Thomas G, Leconet W, Jarlier M, Pugnère M, Vié N, Robert B, Monnet C, Bouayadi K, Kharrat H, Mondon P, Pèlerin A, Chardès T (2013) Anti-HER3 domain 1 and 3 antibodies reduce tumor growth by hindering HER2/HER3 dimerization and AKT-induced MDM2, XIAP, and FoxO1 phosphorylation. *Neoplasia* **15**: 335–347.
- Lin W, Kao HW, Robinson D, Kung HJ, Wu CW, Chen HC (2000) Tyrosine kinases and gastric cancer. *Oncogene* **19**: 5680–5689.
- Lee HS, Lee HK, Kim HS, Yang HK, Kim WH (2003) Tumor suppressor gene expression correlates with gastric cancer prognosis. *J Pathol* **200**: 39–46.
- Nam HJ, Ching KA, Kan J, Kim HP, Han SW, Im SA, Kim TY, Christensen JG, Oh DY, Bang YJ (2011) Evaluation of the antitumor effects and mechanisms of PF00299804, a pan-HER inhibitor, alone or in combination with chemotherapy or targeted agents in gastric cancer. *Mol Cancer Ther* **11**: 439–451.
- Nam SY, Ko YS, Jung J, Yoon J, Kim YH, Choi YJ, Park JW, Chang MS, Kim WH, Lee BL (2011) A hypoxia-dependent upregulation of hypoxia-inducible factor-1 by nuclear factor- κ B promotes gastric tumour growth and angiogenesis. *Br J Cancer* **104**: 166–174.
- Nurwidya F, Takahashi F, Murakami A, Takahashi K (2012) Epithelial mesenchymal transition in drug resistance and metastasis of lung cancer. *Cancer Res Treat* **44**: 151–156.
- Park J, Ko YS, Yoon J, Kim MA, Park JW, Kim WH, Choi Y, Kim JH, Cheon Y, Lee BL (2014) The forkhead transcription factor FOXO1 mediates cisplatin resistance in gastric cancer cells by activating phosphoinositide 3-kinase/Akt pathway. *Gastric Cancer* **17**: 423–430.
- Pei J, Lou Y, Zhong R, Han B (2014) MMP9 activation triggered by epidermal growth factor induced FoxO1 nuclear exclusion in non-small cell lung cancer. *Tumour Biol* **35**: 6673–6678.
- Rosol TJ, Tannehill-Gregg SH, LeRoy BE, Mandl S, Contag CH (2003) Animal models of bone metastasis. *Cancer* **97**: 748–757.
- Sekikawa K, Arends JW, Verstijnen CP, van der Linden E, Dinjens W, Schutte B, Bosman FT (1988) Influence of implantation site on growth, antigen expression and metastatic potential of human colonic cancer HT29 and 5583 xenografts in nude mice. *Invasion Metastasis* **8**: 238–252.
- Shankar J, Messenberg A, Chan J, Underhill TM, Foster LJ, Nabi IR (2010) Pseudopodial actin dynamics control epithelial-mesenchymal transition in metastatic cancer cells. *Cancer Res* **70**: 3780–3790.
- Takamaru H, Yamamoto E, Suzuki H, Nojima M, Maruyama R, Yamano HO, Yoshikawa K, Kimura T, Harada T, Ashida M, Suzuki R, Yamamoto H, Kai M, Tokino T, Sugai T, Imai K, Toyota M, Shinomura Y (2012) Aberrant methylation of RASGRF1 is associated with an epigenetic field defect and increased risk of gastric cancer. *Cancer Prev Res (Phila)* **5**: 1203–1212.
- van der Horst A, Burgering BM (2007) Stressing the role of FoxO proteins in lifespan and disease. *Nat Rev Mol Cell Biol* **8**: 440–450.
- Wu Y, Shang X, Sarkissyan M, Slamon D, Vadgama JV (2010) FOXO1A is a target for HER2-overexpressing breast tumors. *Cancer Res* **70**: 5475–5485.
- Yanagihara K, Takigahira M, Tanaka H, Komatsu T, Fukumoto H, Koizumi F, Nishio K, Ochiai T, Ino Y, Hirohashi S (2005) Development and biological analysis of peritoneal metastasis mouse models for human scirrhous stomach cancer. *Cancer Sci* **96**: 323–332.
- Yoon J, Cho SJ, Ko YS, Park J, Shin DH, Hwang IC, Han SY, Nam SY, Kim MA, Chang MS, Lee HS, Kim WH, Lee BL (2013) A synergistic interaction between transcription factors nuclear factor- κ B and signal transducers and activators of transcription 3 promotes gastric cancer cell migration and invasion. *BMC Gastroenterol* **13**: 29.

This work is published under the standard license to publish agreement. After 12 months the work will become freely available and the license terms will switch to a Creative Commons Attribution-NonCommercial-Share Alike 4.0 Unported License.